Probing top-philic new physics via four-top-quark production*

Qing-Hong Cao(曹庆宏)[1,2,3†] Jun-Ning Fu(付俊宁)[1‡] Yandong Liu(刘言东)[4,5§]
Xiao-Hu Wang(王小虎)[1¶] Rui Zhang(张睿)[6#]

[1]Department of Physics and State Key Laboratory of Nuclear Physics and Technology, Peking University, Beijing 100871, China
[2]Collaborative Innovation Center of Quantum Matter, Beijing 100871, China
[3]Center for High Energy Physics, Peking University, Beijing 100871, China
[4]Key Laboratory of Beam Technology of Ministry of Education, College of Nuclear Science and Technology, Beijing Normal University, Beijing 100875, China
[5]Beijing Radiation Center, Beijing 100875, China
[6]Theoretical Physics Division, Institute of High Energy Physics, Beijing 100049, China

Abstract: We explore constraints on various new physics resonances from four top-quark production based on current experimental data. Both light and heavy resonances are studied in this work. A comparison of the full width effect and narrow width approximation is also presented.

Keywords: top quark, new physics, collider physics

DOI: 10.1088/1674-1137/ac0c6f

I. INTRODUCTION

Despite its rare rate, four top-quark ($t\bar{t}t\bar{t}$) production in hadron collision was discussed even before the discovery of the top quark [1]. The four-top channel is considerably special in the Standard Model (SM) because it involves both the quantum chromodynamics (QCD) and electroweak (EW) interactions, and the strengths of both interactions are comparable. Particularly, owing to the heavy top-quark mass, the Yukawa interaction between the Higgs boson and top quark is fairly large such that the leading electroweak contribution from the Higgs-top interaction is as important as the one from the QCD interaction. These two interactions are more interwoven when one calculates the higher order quantum corrections; consequently, the theoretical prediction of the four-top production cross section is sensitive to the choice of renormalization scale, which demands two or more loop calculations to reduce the theoretical uncertainties [2]. In addition the four-top channel involves complicated kinematics, which enables the interference between the QCD diagrams and heavy EW resonances to yield a sizable contribution. Therefore, the four-top production is a suitable platform to test new physics (NP) beyond the SM.

Furthermore, the four-top channel serves well for probing both the magnitude and CP phase of the top-Higgs interaction without assumptions on the decay of the Higgs boson, e.g. neither the branch ratio of a particular decay mode nor the total decay width of the Higgs boson [3, 4]. Owing to the unprecedented colliding energy and fast accumulation of the integrated luminosity, the Large Hadron Collider (LHC) can measure the $t\bar{t}t\bar{t}$ production [5-7]. For example, the $t\bar{t}t\bar{t}$ signal is observed at the 2.6σ confidence level at the 13 TeV LHC with an integrated luminosity of 137 fb^{-1}, and the CMS collaboration [6] has published new results on the $t\bar{t}t\bar{t}$ cross section,

$$\sigma(t\bar{t}t\bar{t}) = 12.6^{+5.8}_{-5.2}\ \text{fb}, \tag{1}$$

which is consistent with the tree level prediction in the SM, $\sigma(t\bar{t}t\bar{t})_{\text{SM}} = 9.6$ fb. It yields an upper limit of $\sigma(t\bar{t}t\bar{t})$ at the 95% confidence level as $\sigma(t\bar{t}t\bar{t}) \leqslant 22.5$ fb.

Received 20 May 2021; Accepted 18 June 2021; Published online 27 July 2021

* Supported in part by the National Science Foundation of China (11725520, 11675002, 11635001, 11805013, 12075257), the Fundamental Research Funds for the Central Universities (2018NTST09), the funding from the Institute of High Energy Physics, Chinese Academy of Sciences (Y6515580U1) and the funding from Chinese Academy of Sciences (Y8291120K2)

† E-mail: qinghongcao@pku.edu.cn
‡ E-mail: fujunning@pku.edu.cn
§ E-mail: ydliu@bnu.edu.cn, corresponding author
¶ E-mail: xiaohuwang@pku.edu.cn
# E-mail: zhangr@ihep.ac.cn

In this work, we examine the constraint on various NP resonances from the $t\bar{t}t\bar{t}$ production. We consider the top-philic NP model in which the NP resonance (X) couples only to the top quark. The NP contribution to the $t\bar{t}t\bar{t}$ production can either be through the $X\bar{X}$ pair production or through the X production in association with a top-quark pair ($t\bar{t}X$) with a subsequent decay of $X \to t\bar{t}$ or $X \to tt$ as shown in Fig. 1. M and Γ represent the mass and width of the X particle, respectively, and κ_X is the coupling strength of X to the top quark in the top-philic models. The cross section of the $t\bar{t}t\bar{t}$ production can be parametrized as follows:

$$\sigma^{\rm total} = \sigma^{\rm SM}_{t\bar{t}t\bar{t}} + \kappa_X^2 \sigma^{\rm Int}_{t\bar{t}t\bar{t}}(M,\Gamma) + \kappa_X^4 \sigma^{\rm Res}_{t\bar{t}t\bar{t}}(M,\Gamma), \tag{2}$$

where $\sigma^{\rm SM}_{t\bar{t}t\bar{t}}$ ($\sigma^{\rm Int}_{t\bar{t}t\bar{t}}$, $\sigma^{\rm Res}_{t\bar{t}t\bar{t}}$) denotes the cross section of the SM contribution, the interference between the SM and NP, and the NP contribution alone, respectively.

The width dependence in Eq. (2) originates from the propagator of the X particle in the intermediate state. The cross section can be simplified when the X particles are on a mass shell using narrow width approximation (NWA) [8] which enables us to factorize the $t\bar{t}t\bar{t}$ production induced by NP into the X production process and X decay process unambiguously. The interference between the SM and NP contributions is negligible in the vicinity of M; therefore, $\sigma(t\bar{t}t\bar{t})$ can be parametrized as follows:

$$\begin{aligned} X\bar{X} &: \ \sigma(t\bar{t}t\bar{t}) = \sigma(X\bar{X}) \times {\rm Br}^2(X \to t\bar{t}), \\ t\bar{t}X &: \ \sigma(t\bar{t}t\bar{t}) = \sigma(t\bar{t}X) \times {\rm Br}(X \to t\bar{t}). \end{aligned} \tag{3}$$

It should be noted that the resonance X can also decay into a pair of gluons or photons through a top-quark triangle loop in the top-philic model. The loop-induced decays are suppressed by a loop factor $\alpha_s/4\pi$ or $\alpha_e/4\pi$, resulting in small branching ratios $\lesssim 1\%$ for a heavy X. We assume ${\rm Br}(X \to t\bar{t}) = 1$ in the study for simplicity. Therefore, $\sigma(t\bar{t}t\bar{t})$ of the NP process of $pp \to t\bar{t}X \to t\bar{t}t\bar{t}$ can be simplified as follows:

$$\sigma^{\rm NP}_{t\bar{t}X} = \kappa_X^2 \sigma^{\rm Res}_{t\bar{t}X}(M) \times {\rm Br}(X \to t\bar{t}), \tag{4}$$

whereas for the process of $pp \to X\bar{X} \to t\bar{t}t\bar{t}$,

$$\sigma^{\rm NP}_{X\bar{X}} = \sigma^{\rm Res}_{X\bar{X}}(M) \times {\rm Br}^2(X \to t\bar{t}). \tag{5}$$

The absence of κ_X dependence in $\sigma^{\rm NP}_{X\bar{X}}$ is because only gauge interaction is involved in the $X\bar{X}$ pair production.

As the width Γ increases dramatically with κ_X, the width effect can be sizable and the NWA may not be valid. Eqs. (4) and (5) only illustrate the dependence of $\sigma(t\bar{t}t\bar{t})$ on the NP parameters; we keep the width effect of the X particle in our calculation. We adopt the CERN LEP line-shape prescription of a resonance state [9] and express the X propagator as

$$\frac{1}{(p^2 - M^2) + {\rm i}M\Gamma(p^2/M^2)} \tag{6}$$

which makes a distortion on the dispersion relation at the $\Gamma^2/2M^2$ level. A comparison between the full width effect and NWA is presented later.

When the X particle is below the top quark pair mass threshold ($M \leqslant 340$ GeV) or too heavy to be produced directly at the LHC, the X particle in the intermediate state can never be on the mass shell. Therefore, the $t\bar{t}t\bar{t}$ production then depends on κ_X and M,

$$\sigma^{\rm total} = \sigma^{\rm SM}_{t\bar{t}t\bar{t}} + \kappa_X^2 \sigma^{\rm Int}_{t\bar{t}t\bar{t}}(M) + \kappa_X^4 \sigma^{\rm Res}_{t\bar{t}t\bar{t}}(M). \tag{7}$$

For colored resonances, the process in Fig. 1(a) is dominant for a light X because it consists of more Feynman diagrams than the $X\bar{X}$ pair production (b). However, the process in Fig. 1(b) dominates when $m_X > 2m_t$.

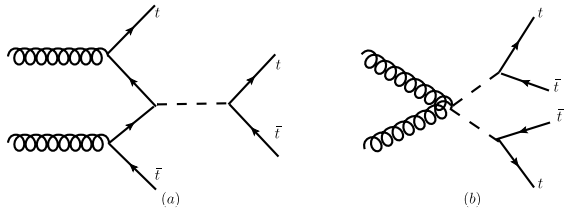

Fig. 1. Pictorial diagrams of $t\bar{t}t\bar{t}$ production in NP models: (a) associated production of $t\bar{t}X$ with $X \to t\bar{t}$; (b) pair production of $X\bar{X}$ with $X \to t\bar{t}$.

II. NEW PHYSICS RESONANCES

Now, consider the LHC search on NP resonances. Rather than focusing on specific NP models, we consider various simplified NP models that extend the SM with an additional NP resonance. The effective Lagrangians are listed as follows:

- A color singlet scalar ($\mathcal{S}$), e.g., [10-12],

$$\mathcal{L} \supset -\bar{t}(a_t + {\rm i}\gamma_5 b_t) t \mathcal{S}, \tag{8}$$

where $a_t = 0$ and $b_t = 0$ corresponds to a CP-odd scalar (A) and a CP-even scalar (H), respectively, and the case of $a_t \neq 0$ and $b_t \neq 0$ represents a CP-mixture scalar;

- a color octet scalar ($\mathcal{S}_8$), e.g., sgluon [13, 14],

$$\mathcal{L} \supset {\rm Tr}[(D_\mu \mathcal{S}_8)^\dagger (D^\mu \mathcal{S}_8)] - \mathcal{S}_8^A \bar{t}(g_8^a + {\rm i}\gamma_5 g_8^b) T^A t, \tag{9}$$

where T^A stands for the $SU(3)_C$ generator;

- a color octet vector ($\mathcal{V}_{8\mu}$), e.g., axigluon [15, 16], color octet boson [17, 18], or *KK* gluon [19],

$$\begin{aligned}\mathcal{L} \supset & -\frac{1}{2}D_\nu \mathcal{V}^A_{8\mu}(D^\nu \mathcal{V}_8^{\mu A} - D^\mu \mathcal{V}_8^{\nu A}) \\ & -\frac{1}{2}g_s f^{ABC} G_{\mu\nu A}\mathcal{V}^B_{8\mu}\mathcal{V}^C_{8\mu} \\ & +\mathcal{V}^A_{8\mu}\bar{t}(g_8^V\gamma^\mu + g_8^A\gamma^\mu\gamma_5)T^A t, \end{aligned} \tag{10}$$

where g_8^V and g_8^A denote the vector and axial vector coupling, respectively;

- a color singlet vector ($\mathcal{V}_\mu$) [20, 21],

$$\mathcal{L} \supset V_\mu \bar{t}(g^V\gamma^\mu + g^A\gamma^\mu\gamma^5)t, \tag{11}$$

where g^V and g^A represent the vector and axial vector coupling, respectively;

- a color sextet and EW singlet scalar $\mathcal{S}_6$ [1)], e.g., color sextet scalar [22-24],

$$\mathcal{L} \supset \mathrm{Tr}[(D_\mu \mathcal{S}_6)^\dagger (D^\mu \mathcal{S}_6)] + g_6 \mathcal{S}_6^A \bar{t}_R \overline{K}^A t_R^C + \mathrm{h.c.}, \tag{12}$$

where K^A stands for the Clebsh-Gordon coefficient.

Equipped with the effective Lagrangians shown above, we can check the validation of the NWA. The decay width of the NP resonances into a pair of top quarks, $\Gamma(X) \equiv \Gamma(X \to t\bar{t})$ or $\Gamma(X \to tt)$, are

$$\Gamma(\mathcal{S}) = \frac{3M}{8\pi}\left[(a_t)^2\beta_t^2 + (b_t)^2\right]\beta_t, \tag{13}$$

$$\Gamma(\mathcal{S}_8) = \frac{3M}{48\pi}\left[(g_8^a)^2\beta_t^2 + (g_8^b)^2\right]\beta_t, \tag{14}$$

$$\Gamma(\mathcal{V}) = \frac{M}{4\pi}\left[(g^V)^2\left(1+2\frac{m_t^2}{M^2}\right) + (g^A)^2\beta_t^2\right]\beta_t, \tag{15}$$

$$\Gamma(\mathcal{V}_8) = \frac{M}{24\pi}\left[(g_8^V)^2\left(1+2\frac{m_t^2}{M^2}\right) + (g_8^A)^2\beta_t^2\right]\beta_t, \tag{16}$$

$$\Gamma(\mathcal{S}_6^A) = \frac{g_6^2 M}{8\pi}\left(1-2\frac{m_t^2}{M^2}\right)\beta_t, \tag{17}$$

where $\beta_t = \sqrt{1-4m_t^2/M^2}$ is the velocity of the top quark. Because the colored resonance exhibits a narrower width in comparison with the color neutral objects, e.g., the width of a color-octet (sextet) resonance is 1/6 (1/3) of a color neutral resonance, we examine the width-to-mass ratio of the color-neutral resonances below.

Figure 2 plots the ratio Γ/M as a function of M for a color singlet scalar (red) and color singlet vector (blue). For demonstration, we choose two sets of coupling parameters. When the strength of its coupling to the top quark is large, a heavy color-singlet scalar exhibits a large width, e.g. $\Gamma/M \simeq 23\%$ in the region of $M \sim 2000$ GeV; see the red-solid curve. However, for such a heavy scalar, the $\sigma(t\bar{t}t\bar{t})$ is highly suppressed such that the large width leads to a mild effect in the constraints on NP resonance. The width effect turns to be sizable in the $t\bar{t}t\bar{t}$ production in the region of $M \sim 800$ GeV. However, the width-to-mass ratio of the colored scalar and vector do not exceed 5% such that the NWA works well and the interference effect can be safely dropped. In this study, we include the full width effect in the calculation to constrain the NP resonance at the LHC, and a comparison of the full width and NWA is presented at the end of the section.

Next, we show the comparison of the four top quark production rates in the simplified models. First, we focus on a light resonance, namely one with mass smaller than $2m_t$, and we fix the mass of 300 GeV. For such a light resonance, it can only contribute to the four top quark production via off-shell effects and its width effect can be neglected in the cross section calculation. This means we can parametrize the cross section in terms of its couplings. We assume that both the SM and NP processes exhibit the same *K*-factor of 1.58 [2]. The cross sections of the $t\bar{t}t\bar{t}$ production induced by the 300 GeV NP resonances at the 13 TeV LHC are given by

$$\begin{aligned}\sigma_{\mathcal{S}}^{\mathrm{total}} =& 9.608 + 1.414(a_t)^2 + 3.999(b_t)^2 \\ & + 3.724(a_t)^4 + 10.771(a_t b_t)^2 + 8.750(b_t)^4, \\ \sigma_{\mathcal{V}}^{\mathrm{total}} =& 9.608 - 7.728(g^V)^2 + 17.394(g^A)^2 \\ & + 34.604(g^V)^4 + 32.648(g^V g^A)^2 + 75.216(g^A)^4, \\ \sigma_{\mathcal{S}_8}^{\mathrm{total}} =& 9.608 + 0.378(g_8^a)^2 + 0.623(g_8^b)^2 \\ & + 1.522(g_8^a)^4 + 6.017(g_8^a g_8^b)^2 + 3.244(g_8^b)^4, \\ \sigma_{\mathcal{V}_8}^{\mathrm{total}} =& 9.608 + 25.895(g_8^V)^2 + 0.412(g_8^A)^2 \\ & + 63.398(g_8^V)^4 + 82.039(g_8^V g_8^A)^2 + 34.292(g_8^A)^4, \\ \sigma_{\mathcal{S}_6}^{\mathrm{total}} =& 9.608 + 0.373(g_6)^2 + 16.435(g_6)^4. \end{aligned}$$

Throughout the paper, all cross sections have the unit of femtobarn (fb). The magnitude of the coefficients before effective coupling combinations reveals the relative size of interference and NP contribution in comparison with the SM prediction (i.e., the constant term in above equation). We also plot the $\sigma(t\bar{t}t\bar{t})$ as a function of effective couplings (denoted by κ_X) in Fig. 3, and for simplicity,

1) The color sextet scalar could be an EW singlet or triplet under $SU(2)_L$, which couples to right-handed or left-handed fermions in the SM, respectively. As an EW triplet and color sextet, the scalar could induce rich collider signatures such as $b\bar{b} \to t\bar{t}$. For simplicity we focus on the case of S_6 being a EW singlet here.

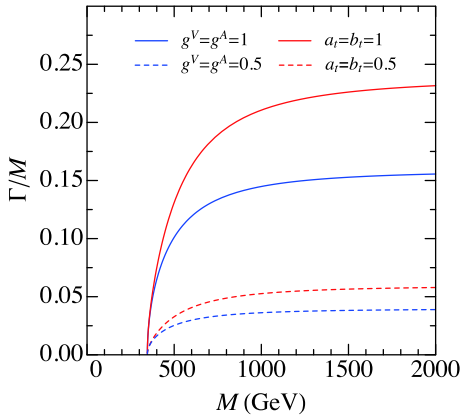

Fig. 2. (color online) Ratio Γ/M as a function of M for a color-neutral scalar (red) and color-neutral vector (blue).

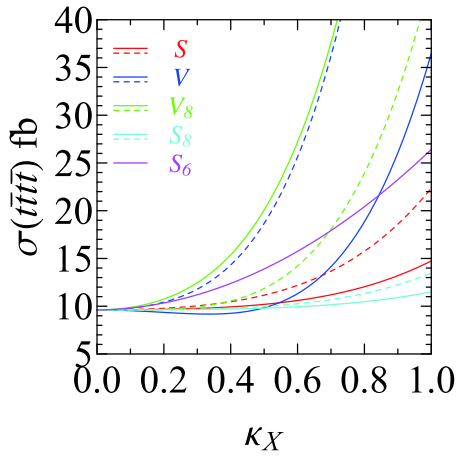

Fig. 3. (color online) The $t\bar{t}t\bar{t}$ production cross section as a function of κ_X in the extended simplified models for $M = 300$ GeV. The solid lines represent the scalar or vector couplings, whereas the dashed curves represent the pseudo-scalar or axial-vector couplings.

we consider one coupling at a time. The solid lines represent the scalar or vector couplings, whereas the dashed curves denote the pseudo-scalar or axial-vector couplings. Obviously, when the coupling approaches 1, the NP contribution alone, i.e., the terms proportional to κ_X^4, tends to dominate the production cross section. For a medium κ_X, the axial-vector and pseudo-scalar couplings enhance the cross section sizably owing to the interference with the SM contribution.

Second, we consider the production of an 800 GeV resonance in the $t\bar{t}t\bar{t}$ production. For a color neutral resonance, the $t\bar{t}t\bar{t}$ production is dominated by the $t\bar{t}X$ association production with $X \to t\bar{t}$; consequently, for a colored resonance, the $X\bar{X}$ pair production through pure QCD with $X \to t\bar{t}$ overwhelmingly dominates the $t\bar{t}t\bar{t}$ production assuming $\mathrm{Br}(X \to t\bar{t}) = 1$. Under the NWA approximation, the $t\bar{t}t\bar{t}$ production cross sections read as

$$\sigma_{\mathcal{S}}^{\rm total} = 9.608 + 5.926(a_t)^2 + 7.076(b_t)^2, \tag{18}$$

$$\sigma_{\mathcal{V}}^{\rm total} = 9.608 + 35.804(g^V)^2 - 1.830 g^V g^A + 35.804(g^A)^2, \tag{19}$$

$$\sigma_{\mathcal{S}_8}^{\rm total} = 189.477 + 20.166(g_8^a)^2 + 19.4288(g_8^b)^2, \tag{20}$$

$$\sigma_{\mathcal{V}_8}^{\rm total} = 6792.253 + 196.729(g_8^V)^2 + 189.482(g_8^A)^2, \tag{21}$$

$$\sigma_{\mathcal{S}_6}^{\rm total} = 349.305 + 63.197(g_6)^2. \tag{22}$$

The cross section depends only on the quadratic power of the effective coupling κ_X because the decay branching ratio of $X \to t\bar{t}$ is assumed to be 1 and independent of κ_X. The constant terms represent the sum of the SM contribution and $X\bar{X}$ production, if applicable.

We then explore the constraints on various top-philic resonances from the recent results of the $t\bar{t}t\bar{t}$ production reported by the CMS collaboration, $\sigma(t\bar{t}t\bar{t}) = 12.6^{+5.8}_{-5.2}$ fb [6]. Because the sensitivity of the $t\bar{t}t\bar{t}$ production to κ_X highly depends on the production channel and the mass of the resonance M, we consider both light and heavy resonances in this study.

We begin with the case of a color singlet vector boson $\mathcal{V}$. Fig. 4(a) shows the allowed parameter region in the plane of (g^A, g^V) for a light color-neutral vector. For illustration, we consider three benchmark masses, 100 GeV (red), 200 GeV (blue), and 300 GeV (yellow). The axial-vector coupling is constrained more than the vector coupling because the axial-vector contribution is enhanced by $m_t^2/m_{\mathcal{V}}^2$ for the light resonance; for example, $|g^A| \lesssim 0.2$ and $|g^V| \lesssim 1$. Figure 4(b) shows the allowed parameter space of a heavy resonance for three benchmark masses, 350 (red), 800 (blue), and 1000 GeV (yellow). The major contribution to the $t\bar{t}t\bar{t}$ production is from the $t\bar{t}\mathcal{V}$ production whose cross section depends on the quadratic power of $g^{V/A}$'s, shown by $\sigma_{\mathcal{V}}^{\rm total}$ for $M = 800$ GeV in Eq. (19). It results in a circle parameter space centering around $g^A = g^V = 0$. The $\sigma(t\bar{t}t\bar{t})$ decreases dramatically with M to weaken the bound; for example, $|g^{V,A}| \lesssim 0.5$ for $M = 1000$ GeV, whereas $|g^{V,A}| \lesssim 0.2$ for $M = 350$ GeV.

Figure 4(c) and (d) show the allowed parameter space for a light and heavy color-neutral scalar $\mathcal{S}$, respectively. First, we observe a similar pattern as the color-neutral vector but with weaker bounds. It should be noted that the contribution of the scalar interaction ($a_t \neq 0$, $b_t = 0$) is suppressed by the top-quark velocity, therefore, the scalar interaction is less constrained. Second, owing to the small production rate, the TeV scalar is loosely bounded, e.g., $\sqrt{a_t^2 + b_t^2} \sim 1.5$, as shown in the yellow region in Fig.

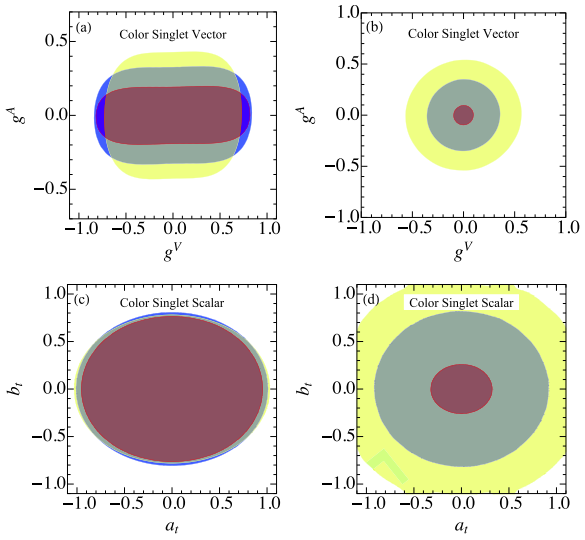

Fig. 4. (color online) Allowed region for a color-neutral vector $\mathcal{V}$ (a, b) and scalar $\mathcal{S}$ (c, d). The red (blue, yellow) region in (a, c) presents the resonance with a mass of 100 (200,300) GeV, respectively, and in (b, d) with a mass of 350 (800, 1000) GeV, respectively.

4(d). The NP scalar exhibits a large width for the large coupling, e.g., $\Gamma/M \sim 30\%$ and cannot be treated as a fundamental particle.

Next, we consider a color octet vector boson $\mathcal{V}_8$. Figure 5(a) plots the allowed parameter space in the plane of (g_8^V, g_8^A) for three benchmark masses of a light $\mathcal{V}_8$. The red (blue, yellow) region in (a) denotes a vector boson with a mass of 100 (200,300) GeV, respectively. The contribution of the axial-vector current interaction in the four-top production is enhanced by $m_t^2/m_{\mathcal{V}_8}^2$; therefore, the lighter the $\mathcal{V}_8$, the larger the $\sigma(t\bar{t}t\bar{t})$. For example, the bound of a 100 GeV vector (red) is much tighter than that of a 300 GeV vector (yellow). However, the enhancement disappears when $m_{\mathcal{V}_8} \sim 300$ GeV and the interference with the SM gluon contribution, i.e., the vector coupling, plays a leading role. As a result, g_8^V is constrained more tightly than g_8^A for a 300 GeV resonance. When the vector boson mass exceeds $2m_t$, because the vector boson carries a color charge, the four top production is dominated by the $\mathcal{V}_8\mathcal{V}_8$ production with a subsequent decay of $\mathcal{V}_8 \to t\bar{t}$. The production rate depends only on the color charge of $\mathcal{V}_8$ but not on g_8^V and g_8^A. The black curve in Fig. 5(b) shows $\sigma(t\bar{t}t\bar{t})$, i.e., $\sigma(\mathcal{V}_8\mathcal{V}_8)$ with $\mathrm{Br}(\mathcal{V}_8 \to t\bar{t}) = 1$, at the LHC. The red line denotes the exclusion bound at the 2σ confidence level, which shows that the mass of $\mathcal{V}_8$ is larger than 1.82 TeV.

Subsequently, we consider a color octet scalar $\mathcal{S}_8$. Figure 6(a) plots the allowed parameter space of g_8^a and g_8^b where the red (blue, yellow) region represents the $\mathcal{S}_8$ mass of 100 (200,300) GeV, respectively. When $m_{\mathcal{S}_8} \sim 300$ GeV, the QCD pair production becomes significant and enlarges the production cross section, yielding

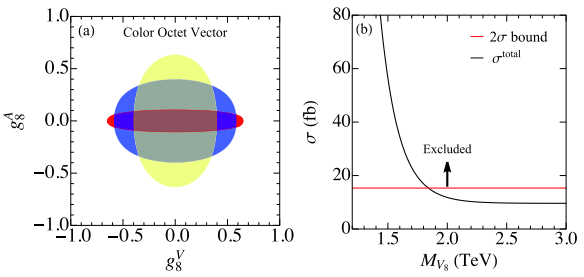

Fig. 5. (color online) Allowed region for a light (a) and heavy (b) color-octet vector boson $\mathcal{V}_8$. The red (blue, yellow) region in (a) denotes a vector boson with mass of 100 (200,300) GeV, respectively. The black curve in (b) denotes $\sigma(t\bar{t}t\bar{t})$ as a function of $m_{\mathcal{V}_8}$, whereas the red curve represents the exclusion limit on $\sigma(t\bar{t}t\bar{t})$ at the 2σ confidence level.

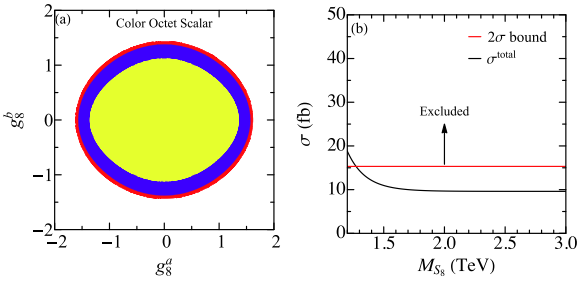

Fig. 6. (color online) Allowed region for a light (a) and heavy (b) color octet scalar $\mathcal{S}_8$. The red (blue, yellow) region represents the mass of 100 (200,300) GeV, respectively. The black curve in (b) denotes $\sigma(t\bar{t}t\bar{t})$ as a function of $M_{\mathcal{S}_8}$, whereas the red curve represents the exclusion limit on $\sigma(t\bar{t}t\bar{t})$ at the 2σ confidence level.

a smaller region, as shown by the yellow oval. When going above the top-quark pair threshold, such as $m_{\mathcal{S}_8} > 2m_t$, the current data demand $m_{\mathcal{S}_8} > 1.19$ TeV; see Fig. 6(b).

Last but not least, we discuss the case of a color sextet scalar $\mathcal{S}_6$ [22-24]. The production depends on $m_{\mathcal{S}_6}$ and g_6. Again, we consider both the light and heavy scalars. Figure 7(a) shows the bound on a light color-sextet scalar where the region above the black curve is excluded by the current data. When $m_{\mathcal{S}_6} > 2m_t$, the $\mathcal{S}_6\mathcal{S}_6^\dagger$ pair production dominates the $t\bar{t}t\bar{t}$ production such that the $\sigma(t\bar{t}t\bar{t})$ does not depend on g_6 at all, as shown by the black curve in Fig. 7(b). To respect the current bound on $\sigma(t\bar{t}t\bar{t})$ (red), the mass of $\mathcal{S}_6$ has to be larger than 1.38 TeV.

Finally, we discuss the difference between the full width effect and NWA. As shown in Fig. 2, for given mass and couplings, the width of a color neutral resonance is larger than that of a colored object, we focus on the color singlet scalar and vector. To emphasize the width effect, we choose a benchmark mass for both the scalar and vector as $M = 800$ GeV. Figure 8 shows the allowed parameter space in the plane of effective couplings for a color neutral scalar (a) and vector (b), where the red solid curve represents the bound with the full width effects, whereas the blue dashed curve represents

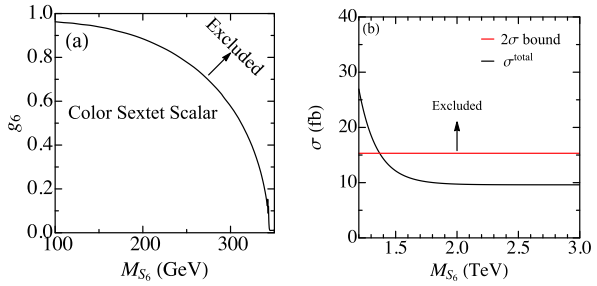

Fig. 7. (color online) Limits on the color sextet scalar coupling and mass from current four top quark production constraints.

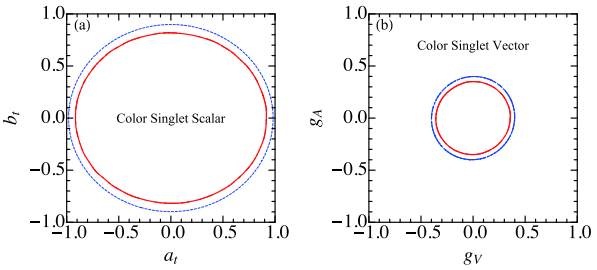

Fig. 8. (color online) Comparison between the full width (red) and NWA (blue dashed): (a) color singlet scalar, (b) color singlet vector. For simplicity, the masses of the scalar and vector are chosen as 800 GeV.

the bound with the NWA. When the full width is incorporated into the calculation, the cross section of the $t\bar{t}t\bar{t}$ production is slightly enlarged to yield a more stringent parameter space.

III. HIGH DIMENSIONAL OPERATORS

In this section we consider two samples of high dimension operators, which contribute to four top quark production. One is the dimension-6 four top-quark operator in composite top-quark models [25-29] in which the right-handed top quark is composite. The four top quark contact operator is [30]

$$O_{t\bar{t}t\bar{t}} = \frac{g_4}{\Lambda^2}(\bar{t}_R\gamma_\mu t_R)(\bar{t}_R\gamma^\mu t_R), \tag{23}$$

where Λ denotes the NP scale. It yields the cross section of $t\bar{t}t\bar{t}$ production as follows:

$$\sigma^{\rm total} = 9.608 - 1.637\, g_4\left(\frac{\rm TeV}{\Lambda}\right)^2 + 4.664\, g_4^2\left(\frac{\rm TeV}{\Lambda}\right)^4, \tag{24}$$

where the constant term denotes the SM contribution, the linear term of g_4 is the interference between the SM and $O_{t\bar{t}t\bar{t}}$, and the quadratic term of g_4 represents the contribution from $O_{t\bar{t}t\bar{t}}$ only. The pure QCD corrections to the interference and quadratic term are calculated in [31], namely 0.57 and 0.93, respectively. We obtain a constraint on the g_4 coupling from the current data as

$$-1.34 < g_4\left(\frac{\rm TeV}{\Lambda}\right)^2 < 1.55. \tag{25}$$

The other sample is the top quark dipole operator given by [32]

$$\mathcal{L} \supset \frac{g_s}{m_t}\bar{t}T^A(d_V + {\rm i}d_A\gamma_5){\rm i}\sigma_{\mu\nu}tG^{\mu\nu A}, \tag{26}$$

where $\sigma_{\mu\nu} \equiv [\gamma_\mu,\gamma_\nu]/2$. The dipole operator interferes with the SM diagram in a complex manner. For example, its interference between the electric dipole operator and SM depends mainly on the even power of the Wilson coefficient because the electric dipole operator violates the CP parity. Thus, it yields a symmetric bound on d_A. However, the interference between the magnetic dipole operator and SM depends on the odd power of the Wilson coefficient and yields an asymmetric constraint on the d_V. Figure 9 shows the allowed parameter space in the plane of d_V and d_A with respect to the current LHC data.

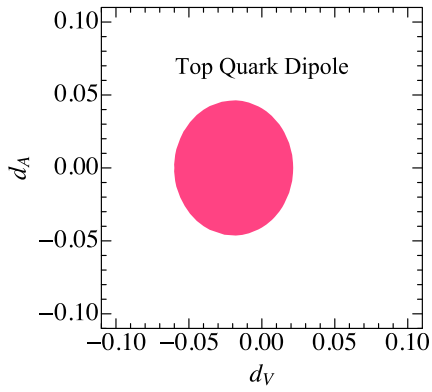

Fig. 9. (color online) Allowed region for the Wilson coefficients of the top color electric dipole operator and color magnetic dipole operator.

IV. A BROAD RESONANCE

Finally, we evaluate a special case of a broad vector resonance ρ^μ proposed in Ref. [33]. The resonance decays mainly into a pair of top or bottom quarks, and the Lagrangian reads

$$\mathcal{L} \supset g_t(\bar{t}_L\gamma_\mu t_L - \bar{b}_L\gamma_\mu b_L)\rho^\mu, \tag{27}$$

where the coupling g_t describes strong dynamics and can be fairly large. Such a large g_t inevitably generates a very broad width of ρ^μ. It is necessary to modify the Breit-Wigner distribution of the ρ^μ propagator to take care of

the broad width. We modify the broad resonance propagator using the CERN LEP line-shape scheme [9]. To be distinct from the previous study of the NP resonance with a narrow width, we focus on the large g_t and broad width here. Figure 10 shows the exclusion limit of g_t as a function of M_ρ, which shows that g_t increases with M_ρ linearly for a heavy ρ with a mass of several TeVs. This is because the heavy resonance contribution to the $t\bar{t}t\bar{t}$ production depends on the quadratic and quartic powers of coupling-mass-ratio, e.g., g_t/M_ρ, after utilizing the modified propagator.

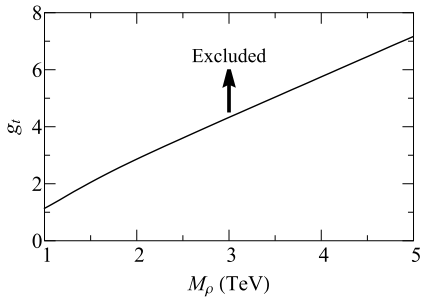

Fig. 10. Excluded parameter region for the broad vector resonance model. Only the large coupling region is shown.

V. DISCUSSION AND CONCLUSION

Despite the rare rate at the LHC, four-top production is the best channel to probe the so-called top-philic resonances that couple only to top quark. We studied various new physics resonances and, based on the current data at the LHC, explored the constraints on the mass of the new resonance and the effective coupling of the new resonance to the top quark. When the effective coupling is small, one can use narrow width approximation to simplify the study. However, when the coupling is large, the width effect is no longer negligible. A comparison of the full width effect and narrow width approximation is made in the study of the color-neutral scalar and vector. A special case of a strong dynamics model is also addressed.

Note added: While finalizing the manuscript, an informative work dealing with the same topic was found online [34].

References

[1] V. D. Barger, A. L. Stange, and R. J. N. Phillips, Phys. Rev. D **44**, 1987-1996 (1991)
[2] R. Frederix, D. Pagani, and M. Zaro, JHEP **02**, 031 (2018), arXiv:1711.02116[hep-ph]
[3] Q. H. Cao, S. L. Chen, and Y. Liu, Phys. Rev. D **95**(5), 053004 (2017), arXiv:1602.01934[hep-ph]
[4] Q. H. Cao, S. L. Chen, Y. Liu *et al*., Phys. Rev. D **99**(11), 113003 (2019), arXiv:1901.04567[hep-ph]
[5] A. M. Sirunyan *et al*. (CMS]), Eur. Phys. J. C **78**(2), 140 (2018), arXiv:1710.10614[hep-ex]
[6] A. M. Sirunyan *et al*. (CMS), Eur. Phys. J. C **80**(2), 75 (2020), arXiv:1908.06463[hep-ex]
[7] M. Aaboud *et al*. (ATLAS), Phys. Rev. D **99**(5), 052009 (2019), arXiv:1811.02305[hep-ex]
[8] H. Pilkuhn, *The Interactions of Hadrons*, (NorthHolland, Amsterdam, 1967)
[9] Q. H. Cao and C. P. Yuan, Phys. Rev. Lett. **93**, 042001 (2004), arXiv:hepph/0401026[hep-ph]
[10] P. S. Bhupal Dev and A. Pilaftsis, JHEP **12**, 024 (2014) [Erratum: JHEP **11**, 147 (2015)] arXiv: 1408.3405 [hepph]
[11] E. Alvarez, D. A. Faroughy, J. F. Kamenik *et al*., Nucl. Phys. B **915**, 19-43 (2017), arXiv:1611.05032[hep-ph]
[12] E. Alvarez, A. Juste, and R. M. S. Seoane, JHEP **12**, 080 (2019), arXiv:1910.09581[hep-ph]
[13] S. Calvet, B. Fuks, P. Gris *et al*., JHEP **04**, 043 (2013), arXiv:1212.3360[hep-ph]
[14] L. Darmé, B. Fuks, and M. Goodsell, Phys. Lett. B **784**, 223-228 (2018), arXiv:1805.10835[hep-ph]
[15] O. Antunano, J. H. Kuhn, and G. Rodrigo, Phys. Rev. D **77**, 014003 (2008), arXiv:0709.1652[hep-ph]
[16] R. S. Chivukula, E. H. Simmons, and C. P. Yuan, Phys. Rev. D **82**, 094009 (2010), arXiv:1007.0260[hep-ph]
[17] P. Ferrario and G. Rodrigo, Phys. Rev. D **78**, 094018 (2008), arXiv:0809.3354[hep-ph]
[18] J. A. Aguilar-Saavedra and J. Santiago, Phys. Rev. D **85**, 034021 (2012), arXiv:1112.3778[hep-ph]
[19] M. Guchait, F. Mahmoudi, and K. Sridhar, Phys. Lett. B **666**, 347-351 (2008), arXiv:0710.2234[hep-ph]
[20] N. Greiner, K. Kong, J. C. Park *et al*., JHEP **04**, 029 (2015), arXiv:1410.6099[hepph]
[21] J. H. Kim, K. Kong, S. J. Lee *et al*., Phys. Rev. D **94**(3), 035023 (2016), arXiv:1604.07421[hep-ph]
[22] C. R. Chen, W. Klemm, V. Rentala *et al*., Phys. Rev. D **79**, 054002 (2009), arXiv:0811.2105[hep-ph]
[23] E. L. Berger, Q. H. Cao, C. R. Chen *et al*., Phys. Rev. Lett. **105**, 181802 (2010), arXiv:1005.2622[hep-ph]
[24] H. Zhang, E. L. Berger, Q. H. Cao *et al*., Phys. Lett. B **696**, 68-73 (2011), arXiv:1009.5379[hep-ph]
[25] E. Eichten, K. D. Lane, and M. E. Peskin, Phys. Rev. Lett. **50**, 811-814 (1983)
[26] B. Lillie, J. Shu, and T. M. P. Tait, JHEP **04**, 087 (2008), arXiv:0712.3057[hep-ph]
[27] A. Pomarol and J. Serra, Phys. Rev. D **78**, 074026 (2008), arXiv:0806.3247[hepph]
[28] K. Kumar, T. M. P. Tait, and R. Vega-Morales, JHEP **05**, 022 (2009), arXiv:0901.3808[hep-ph]
[29] N. Zhou, D. Whiteson, and T. M. P. Tait, Phys. Rev. D **85**, 091501 (2012), arXiv:1203.5862[hep-ph]
[30] C. Zhang, Chin. Phys. C **42**(2), 023104 (2018), arXiv:1708.05928[hep-ph]
[31] C. Degrande, G. Durieux, F. Maltoni *et al*., Phys. Rev. D **103**(9), 096024 (2021), arXiv:2008.11743[hep-ph]
[32] M. Malekhosseini, M. Ghominejad *et al*., Phys. Rev. D **98**(9), 095001 (2018), arXiv:1804.05598[hep-ph]
[33] D. Liu, L. T. Wang, and K. P. Xie, Phys. Rev. D **100**(7), 075021 (2019), arXiv:1901.01674[hep-ph]
[34] L. Darmé, B. Fuks, and F. Maltoni, arXiv: 2104.09512 [hep-ph]